

Cross Sections for the Reactions $D(d,p)T$, $D(d,n)He^3$, $T(d,n)He^4$, and $He^3(d,p)He^4$ below 120 keV*

W. R. ARNOLD,† J. A. PHILLIPS, G. A. SAWYER, E. J. STOVALL, JR., AND J. L. TUCK
Los Alamos Scientific Laboratory, University of California, Los Alamos, New Mexico

(Received August 31, 1953)

These cross sections were measured by the process of passing a deuteron beam into a thin gas target contained behind a thin window of evaporated silicon monoxide. The energy loss in the window was measured by a deceleration technique. Charged particles from the reactions were observed at 90° in the laboratory system with proportional counters. Some results are as follows: for the reaction $D(d,p)T$, by use of the angular distribution reported by Wenzel and Whaling, the total cross section σ is 15.4 mb with a probable error of 3.2 percent at 100-keV incident deuteron energy; $\sigma = 0.629 \text{ mb} \pm 5 \text{ percent}$ at 25 keV. For the reaction $D(d,n)He^3$, $\sigma = 15.2 \text{ mb} \pm 3.2 \text{ percent}$ at 100 keV; $\sigma = 0.592 \text{ mb} \pm 5 \text{ percent}$ at 25 keV. The sum of these two cross sections follows a Gamow function below 50 keV. For the reaction $T(d,n)He^4$, isotropy in the center-of-mass system being assumed, σ shows a peak value of 4.95 barns $\pm 2.8 \text{ percent}$ at 107 keV; at 40 keV, $\sigma = 0.72 \text{ barn} \pm 3.2 \text{ percent}$; at 19 keV, $\sigma = 0.045 \text{ barn} \pm 5 \text{ percent}$; below 19 keV, σ follows a Gamow function. For the reaction $He^3(d,p)He^4$ with isotropy assumed, $\sigma = 16 \text{ mb} \pm 3 \text{ percent}$ at 93 keV; $\sigma = 0.124 \text{ mb} \pm 5 \text{ percent}$ at 36 keV; and σ follows a Gamow relation below 100 keV.

INTRODUCTION

A DETERMINATION of the reaction cross sections for the reactions $D(d,p)T$, $D(d,n)He^3$, $T(d,n)He^4$, and $He^3(d,p)He^4$ at deuteron bombarding energies below 120 keV was considered to be of general interest. At the time this investigation was started in the fall of 1950, the $D(d,p)T$ cross section was known below 100-keV deuteron bombarding energy from thick target measurements¹ by use of an uncertain value for the stopping power of heavy ice and from a brief advance report of results using a thin target method.² The cross section for the neutron branch depended upon the same measurements and upon the branching ratio measurements of Pepper,³ McNeill, Thonemann and Price,⁴ and McNeill and Keyser.⁵ Recently, the reaction cross section and angular distribution for $D(d,p)T$ have been reported on more fully by Moffatt, Roaf, and Sanders,⁶ who provide independent data, and by Wenzel and Whaling,⁷ whose work was carried out in coordination with the present work.

The cross section for the reaction $T(d,n)He^4$ has been measured previously⁸ but the results were not entirely consistent with measurements at higher energies.⁹ Several measurements of the cross section for the

reaction $He^3(d,p)He^4$ have been made,¹⁰ but no measurement at deuteron energies below 100 keV was known to the authors.

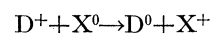
The measurement of these cross sections presented several problems which are peculiar to the low-energy range. These may be summarized as follows:

(1) σ is a steep function of energy. At 20 keV, a 100-v change in energy causes a 2 percent change in cross section for $T(d,n)He^4$, while at 10 keV, 100 v of change cause a 6 percent change in cross section.

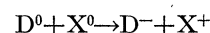
(2) The stopping power of most substances passes through a maximum in the region of 50- to 100-keV deuteron energy so that, combined with (1) above, even monatomic layers of contamination on targets can introduce significant error.

(3) At the time when these considerations arose (1950), the stopping power for likely target materials was certainly not known to within ± 20 percent at these low energies.

(4) The cross sections for the charge-exchange reactions



and



become large when the velocity of the beam deuteron approaches the velocity of an orbital electron, which is the energy range of the present experiment. The charge-exchange cross section approximates molecular dimensions (10^{-16} cm^2). Thus the beam current measurement can be complicated by exchange with the normally negligible residual gas in high vacuums.

When this experiment was being planned, it seemed that thick target methods were ruled out by (3), since

¹⁰ Baker, Holloway, King, and Schreiber, U. S. Atomic Energy Commission Declassified Report No. 2189, 1948 (unpublished); J. Hatton and G. Preston, *Nature* **164**, 143 (1949); Lillie, Bonner, and Conner, *Phys. Rev.* **86**, 630 (1952); Yarnell, Lovberg, Stratton, and Stratton, *Phys. Rev.* **88**, 158 (1952).

* Work performed under the auspices of the U. S. Atomic Energy Commission.

† Now at Schlumberger Oil Well Prospecting Company, Ridgefield, Connecticut.

¹ Bretscher, French, and Seidl, *Phys. Rev.* **73**, 815 (1948).

² Sanders, Moffatt, and Roaf, *Phys. Rev.* **77**, 754 (1950).

³ T. P. Pepper, *Can. J. Research* **27A**, 143 (1949).

⁴ McNeill, Thonemann, and Price, *Nature* **166**, 28 (1950).

⁵ K. G. McNeill and G. M. Keyser, *Phys. Rev.* **81**, 602 (1951).

⁶ Moffatt, Roaf, and Sanders, *Proc. Roy. Soc. (London)* **A212**, 220 (1952).

⁷ W. Wenzel and W. Whaling, *Phys. Rev.* **88**, 1149 (1952).

⁸ E. Bretscher and A. P. French, *Phys. Rev.* **75**, 1154 (1949); D. L. Allan and M. J. Poole, *Proc. Roy. Soc. (London)* **A204**, 500 (1951).

⁹ T. W. Bonner, *Proc. Harwell Nuclear Physics Conf.* (September, 1950); Argo, Taschek, Agnew, Hemmendinger, and Leland, *Phys. Rev.* **87**, 612 (1952).

in such cases

$$\sigma = (dY/dE) \cdot (dE/dx).$$

On the other hand, thin targets could be made so that the error introduced by an uncertainty in dE/dx by, say, 20 percent introduced an inappreciable error. This result called for a target density in the region of 10^{-5} g/cm², and, in such a case, we obtain the cross section

$$\sigma = N / (n_1 n_2 l \Omega),$$

where N = number of disintegrations, n_1 = number of bombarding particles from the beam current, n_2 = target density in particles/cm², l = beam-path length in the target, and Ω = the counting system solid angle. Although it was perfectly possible to obtain films of, say, tritiated ice or tritiated zirconium of sufficient thinness, the problem of estimating n_2 in such films seemed unattractive for an absolute experiment, and, in addition, backscattering of particles from the support which such films require was a further complication.

A thin target consisting of several centimeters of path in gas at 1-mm pressure seemed ideal for precise determination of n_2 and l , n_2 being defined by the readily measurable gas composition, pressure, and temperature and l being large enough for direct measurement.

Such gas targets are commonly operated by admitting the beam through an aperture from the high-vacuum region and disposing of the outflowing gas by a fast differential pumping system. However, at the low energies reason (4) rules against this: the pressure in the antechamber, combined with the large charge-exchange cross section, makes the beam current measurement untrustworthy. Moffatt, Roaf, and Sanders⁸ avoided this difficulty by abandoning measurement of beam current and measuring beam power calorimetrically.

The solution adopted here was to interpose a thin window between the gas target and the high vacuum. The problem then became one of knowing the energy loss in this window with sufficient accuracy and correcting for the scattering and straggling in the beam produced by the window.

Although in principle it was possible to correct for any degree of scattering and straggling, such corrections impaired the reliability of the results, and in designing this experiment our aim was to keep the total magnitude of such corrections below the planned probable error of

6 percent. The requirement that the scattering correction be less than 6 percent proved equivalent to the requirement that half the beam be included within an angle of 5°, or, for 20-kev deuterons in window material with an atomic number in the region of 13(Al), a thickness of 10 μg/cm². The straggling correction depended on the curvature of the σ vs E curve and was most serious at the lowest energies. We found, for example, from the measured σ vs E curve for T(d, n)He⁴ that at 20 kev, if $\Delta\sigma$ is the error, $\Delta\sigma/\sigma = 0.4\delta(E)/E$, where $\delta(E)$ is the root-mean-square deviation in the straggling. Hence $\delta(E)$ must be <3 kev for a correction <6 percent.

It proved possible to develop windows fulfilling these requirements. They consisted of evaporated films of SiO₂ of thickness about 7 μg/cm² (not known precisely), with capability to withstand 1-mm gas pressure on a diameter of 8 mm, of substantial durability under bombardment by 1 μa of deuterons, and with sufficient constancy in thickness. A characteristic film has a mean energy loss of 5 kev at 30 kev, straggling of ±0.4 kev, and average scattering angle of 5°. The films have been discussed elsewhere.¹¹

The beam current was determined by measurement of the charge accumulated by the target chamber and window as a whole. The beam-defining apertures and guard rings were maintained in a high vacuum so that the guard rings could be effective and the charge exchange small.

Other considerations taken into account in the experiment were:

(1) Error in the target density, n_2 , produced by (a) Temperature differences between manometer and target chamber; (b) Local change of gas density produced by heating which resulted from passage of the beam or from contact with the hot window. This effect might be detected by an apparent change of σ with a change in beam current. None was found.

(2) Repassage of beam particles through the target volume caused by backscattering in the rear of the chamber. This effect turned out to be negligible on account of the combination of steep fall-off of σ with E and the small angle subtended by the target volume from the rear of the chamber.

EXPERIMENTAL PROCEDURE

Accelerator

The high voltage, supplied by a conventional Cockcroft-Walton voltage doubler, was fed through a surge resistor to a box containing the probe and focus voltage supplies. The center of the two-gap accelerating tube was tied through surge resistors to the half-voltage point.

The apparatus is shown schematically in Figs. 1 and 2.

The high voltage was measured by means of a series

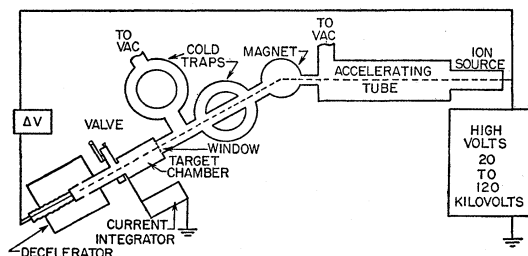


FIG. 1. Cross-section apparatus.

¹¹ G. A. Sawyer, Rev. Sci. Instr. 23, 604 (1952).

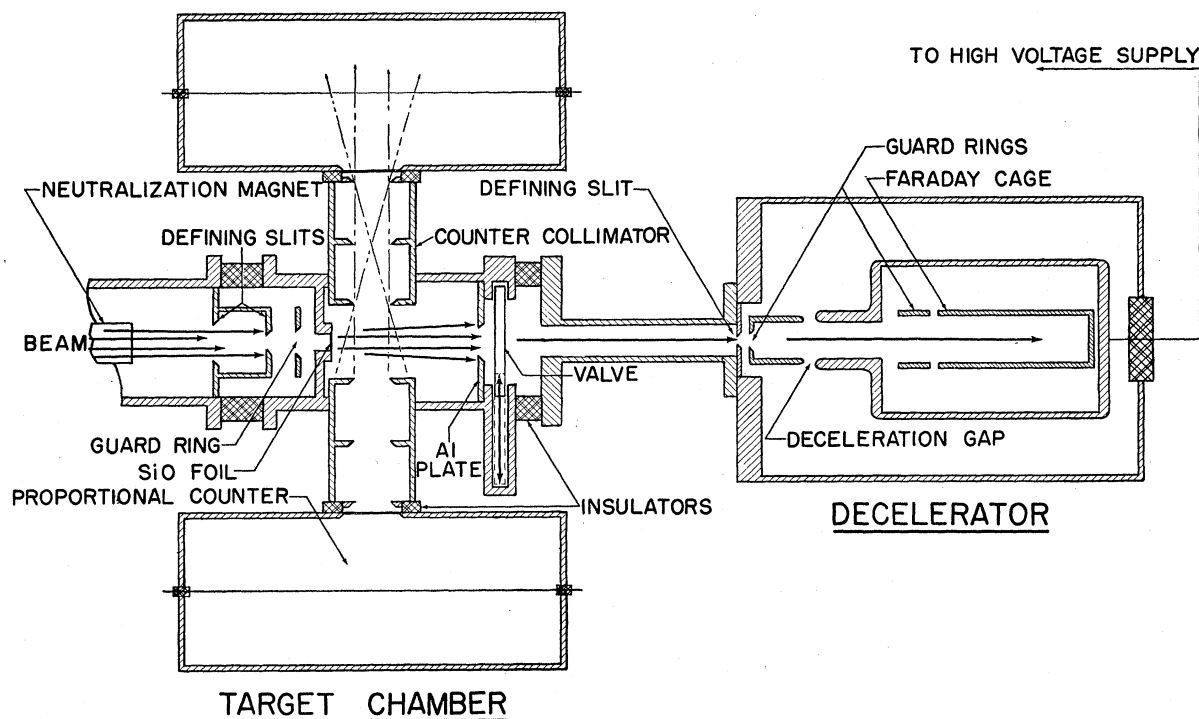


FIG. 2. Target chamber and decelerator for the measurement of low-energy cross sections.

of 30 high-voltage resistors (Shallcross Type 505) of 5 megohms each, rated at 7.5 kv each. The total resistance of the resistors was measured in the Los Alamos Standards Laboratory and fell well within the 0.1 percent accuracy specified by the manufacturer. A type *K* potentiometer measured the potential drop across a 1000-ohm standard resistor at the bottom of the stack. The high-resistance stack was checked for linearity and corona by applying twice the working gradient. No deviation exceeding 0.05 percent was found.

The top of the high-voltage measuring stack was connected to the anode of the ion source (which had the potential closest to that of the ions). The ions started out at a potential slightly below this, and the necessary correction will be discussed under "Energy of Beam in Target."

The ripple on the high voltage, when all parts of the apparatus were functioning, was calculated to be 1 v/kv and checked by measurement to be of this order.

The high voltage was held constant manually, and it was possible to hold the drifts in the high voltage to less than 50 v.

The rf-ion source was copied from the Oxford source.¹² This ion source with plasma focusing and magnetic excitation yielded more than 90 percent of the total beam as D^+ .

¹² Thonemann, Moffat, Roaf, and Sanders, Proc. Phys. Soc. (London) 61, 483 (1948).

Energy of Beam in Target

The energy of the ion beam in the target chamber differed from the energy represented by the high-voltage measurement by (a) a small-voltage drop (~ 100 v) between the ion-source anode and the ion plasma in the ion source, (b) a much larger loss of energy (~ 5 kev) in the thin window of the target chamber, and (c) an energy loss of the order of 300 ev in the target gas. A decelerator was used to measure the energy of the ions after they passed through the window and, hence, to measure (a) and (b), whereas (c) was evaluated by a separate measurement of dE/dx in the target gas.

A gate valve at the rear of the target chamber could be opened when the chamber was evacuated to allow the beam, degraded in energy by the thin window, to pass into the decelerating gap of the decelerator of Fig. 2. The accelerator high voltage conveniently provided the main deceleration potential. Since the deuterons of the beam had lost some energy, this voltage was too high and had to be reduced an amount ΔV equal to the amount of energy lost in the film before the deuterons were able to reach the collector of the decelerator.

In operation, deceleration curves such as those in Fig. 3 were obtained. The "no-foil" curve shows that the energy spread of the beam was about 100 ev, and the average energy of the ions about 100 ev below the high-voltage reading. Since these amounts were included in the deceleration curve which was obtained with an SiO window in place, they were included in the differ-

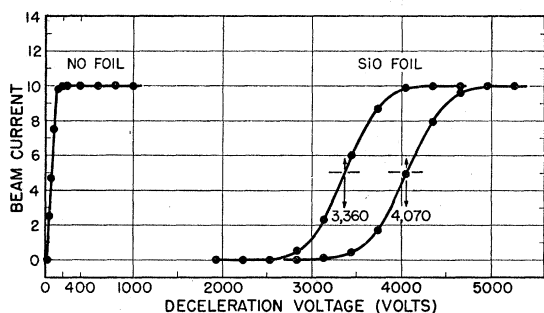


FIG. 3. Typical deceleration curves for no foil and for two SiO foils.

ential voltage, ΔV , subtracted from the high potential to obtain the energy of the ions in the target chamber, and were of importance only if they changed between a deceleration and a run. The constancy of these ion-source drops was checked carefully and found to be a function only of the ion-source gas pressure, which was held constant during cross-section measurements.

The type of deceleration curves obtained with an SiO window is shown to the right in Fig. 3. One foil shown had an average thickness of 3360 ev, along with straggling of about 500 ev. The straggling will be discussed later under SiO foils.

During a deceleration of the positive ions in the measurement of the thickness of a foil, any negative ions caused by charge exchange in the window would, of course, be accelerated. Thus, when the voltage of the decelerator was such as to collect no positive ions, the reading on the electrometer would be an indication of the number of negative ions. The small negative current observed was assumed constant throughout the deceleration since there was no change in the electrometer reading as the deceleration voltage was varied (except when positive ions were being collected).

Although charge equilibrium would be expected to have been reached in the window, there was a possibility that the negative ions did not have the same energy distribution as the positives. We removed this doubt by running the machine at low incident voltages, reversing the polarity of the voltage supply in the decelerator, and decelerating the negative ions. When corrections were made for the biasing voltages on the guard rings, the loss of energy resulting from passage of both positive and negative ions through the foil was found to be the same.

The decelerator received and measured the energy of only that part of the beam within a cone of semiangle 0.8° . The more widely singly-scattered particles had on the average less energy both from having traversed more window thickness and from nuclear scattering through a larger angle. At 25-keV deuteron energy and with an SiO window having a mean energy loss of 5 keV, these effects amounted to 15 and 20 ev, respectively, at a scattering angle of 6° and were thus not serious. However, at lower energies, they became serious and

contributed to a fall-off in the accuracy of the experiment.

The energy loss in SiO windows as a function of energy was measured carefully, and this variation with energy is shown in Fig. 4. Thus, although a given series of runs was made at a variety of energies, it was necessary only to decelerate at one energy before and after the series to be able to calculate the energy loss at other energies.

The energy loss in SiO windows increased slowly during bombardment: to allow for this growth, we made studies of its characteristics, and it proved justifiable to interpolate the growth in terms of the charge passed by the window, provided beam intensities were held reasonably constant, that the gas pressures were normal, and that the total growth from start to finish stayed less than 500 ev.

Although the target was thin, the energy loss of the deuterons in passing through the gas from the window to the axis of the collimators was large enough to need a correction, especially at the lower energies. dE/dx values measured with the decelerator¹³ were used to make this correction (Fig. 5). The energy loss in the gas target was about 300 ev.

Vacuum System

After passing through the probe channel of the ion source, the beam passed through two focusing gaps used to obtain the desired diffuse beam on the target-chamber window. It then proceeded through two accelerating gaps to an analyzing magnet which deflected the desired mass-2 beam through 30° . The operating pressure in this part of the system ran at about 12×10^{-6} mm Hg. The beam then passed through an 8-in. section of $\frac{3}{4}$ -in. diameter tubing held at liquid

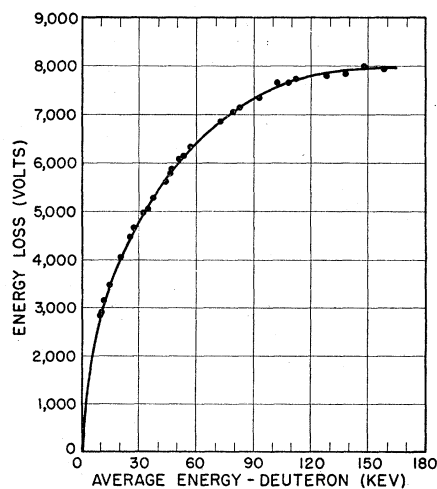


FIG. 4. Energy loss as a function of energy for a typical SiO foil. The curve shown is the average of many SiO foils normalized to a typical energy-loss scale.

¹³ J. A. Phillips, Phys. Rev. **90**, 532 (1953).

air temperatures and with $\frac{3}{8}$ -in. diameter diaphragms at each end. This liquid-air trap removed condensable vapors near the window. The beam then emerged into the "clean" part of the apparatus where great pains were taken to eliminate, as far as possible, sources of condensable vapors which would lead to an increase in the thickness of the target-chamber window. Lead gaskets were used in this region instead of Neoprene O-rings. A side arm pumping system was also used at this point to reduce the pressure to 4×10^{-6} mm Hg and thereby reduce the amount of beam neutralization.

Target Chamber

The target chamber is shown in detail in Fig. 2. The beam entered at the left through the deflecting magnet (used to measure neutralization), the 5-mm diameter collimating hole, and the electron-suppressing guard ring. The beam then impinged on the 8-mm diameter SiO entrance window of the target chamber. At the right the target chamber was closed by a vane-type valve which could be opened to admit the beam to the decelerator. Glass insulators were used to insulate the target chamber from the accelerator tube and decelerator whereas thin mica rings insulated the target chamber from the counters. The target chamber was insulated so the beam current to it could be measured.

Target Atoms

Since a gas target was used, the calculation of the number of target atoms per cubic centimeter depended upon measurement of pressure, temperature, and purity.

A. Pressure

Measurement of pressure was complicated by the requirement that condensable vapors in the target chamber be kept to an absolute minimum, for reasons that will be discussed below under "Purity." This condition ruled out the use of oil or mercury manometers in direct contact with the tritium gas in the target chamber. Instead, a Consolidated Engineering Company micromanometer was used to measure tritium gas pressure. The micromanometer was not absolute and had to be calibrated with a fluid manometer.

The micromanometer has a diaphragm which is deformed by the pressure to be measured, changing the capacity between the diaphragm and a fixed plate. This capacity is in one arm of a capacity bridge which may be balanced by placing a standard variable condenser in another arm and adjusting to balance. This micromanometer was designed originally to work over the pressure range 1–100 μ , and modification of the bridge was required for the pressure range 1–1000 μ . As ordinarily used, the manometer was found to be subject to zero shifts and temperature effects. It proved necessary to follow a strict procedure in applying pressures to the gauge to eliminate the zero shifts and to control the temperature of the gauge to 0.1°C by a

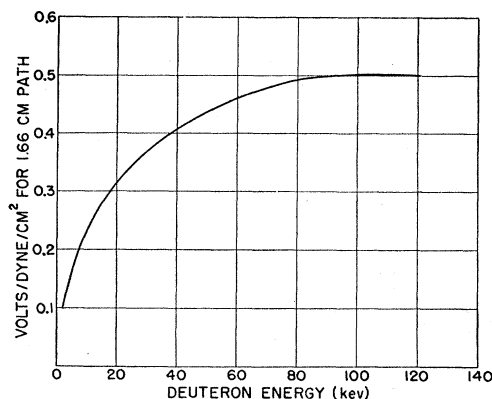


FIG. 5. Energy loss in hydrogen as a function of energy.

thermostat to eliminate the temperature effects. The measuring bridge gave readings of the pressure in the 1000- μ region to 1 part in 1000.

The fluid manometer used for calibration consisted of a U-tube constructed of 1-cm bore precision glass tubing. Collimated light from two sources striking the respective menisci were viewed through two microscopes mounted on a vertical cathetometer. The cross hairs were set on the first dark line of the diffraction pattern produced at the fluid-air interface, and the setting was very reproducible. The calibration of the gauge was checked periodically throughout the series of runs and did not vary by more than ± 0.3 percent throughout. It was necessary to calibrate at the end of a day's running so that the manometer vapor introduced into the gauge during calibration could be pumped out overnight. Analytical quality butyl phthalate was used as the manometer fluid, and, as a precaution against errors of composition, its density was measured over a range of temperatures with a standardized pycnometer.

B. Temperature

Two measurements were made: (1) the temperature of the target chamber body as read by a thermometer, and (2) the temperature difference between the gas and the chamber body as measured by a fine wire thermocouple in the gas. Use of the thermocouple was discontinued after no temperature difference was observed between gas and chamber body.

C. Purity

Attainment of purity proved to be one of the major difficulties in the experiment. Tritium was supplied from a small uranium reservoir and after use was collected into another uranium trap. About one-third of the gas from each filling was taken as a sample for analysis. The tritium gas was analyzed on a mass spectrometer before and after use. However, the gas sample was collected at about 800 to 1000 dynes/cm² (about $\frac{2}{3}$ -mm Hg) and then compressed by a Toeplitz

pump to 1 cm Hg during the mass analysis. For this reason a condensable vapor might not have been detected. One check on condensable hydrocarbons was to look at the CT_4 mass spot in the mass spectrometer since CT_4 would be formed from hydrocarbons in an ionized tritium atmosphere. Very small amounts of CT_4 were observed, but there was no way of getting a quantitative check on hydrocarbons.

The method used for condensable vapors was to try to eliminate rather than measure them. It was found during the first runs that the measured yield fell, with time, about twice as fast as could be accounted for by growth of the target window and was frequently an erratic function of pressure changes caused by adding or removing part of the tritium. The difficulty was apparently caused by an increase in the partial pressure of oil vapors which started building up the moment the target chamber was isolated. Such a rise in pressure could be noted on the Consolidated gauge and was much worse immediately after calibration (which involved exposing the systems to fluid vapors).

The pressure rise was reduced to less than 0.3 dyne/cm² min at pressures of less than 5 dynes/cm² in the target chamber by pumping at least overnight after calibration. Although this rate of rise extrapolates to predict a 2 percent drop/hr in cross section, the drop actually observed was in almost all cases less, indicating that vapor reached an equilibrium pressure.

The gas entered the target as 99.5 percent tritium plus 0.5 percent hydrogen, and the mass analysis after running was usually about 96 percent T, 2 percent H, 2 percent N. The absence of oxygen to go with the nitrogen indicated that air had entered the chamber during the run instead of during handling of the sample and that the oxygen had been converted to T_2O in the ionized target gas. The T_2O could not be measured on the mass spectrometer because of background difficulties. However, water vapor (T_2O) was not a cause of error since the number of tritium atoms per unit pressure is the same as for T_2 gas. The increase in hydrogen was undoubtedly the result of exchange of tritium with hydrogen in hydrocarbons on the chamber walls. At very low deuteron energies (below 20 kev), the rate of hydrogen contamination of the tritium was greatly increased, possibly because of widely scattered beam particles striking the Gelva (polyvinyl acetate) used to anchor the collimator slits in the collimator tube. This was one of several factors which decreased the accuracy of the very low energy measurements.

Thin SiO Window

The foil window at the entrance to the target chamber served to contain the target gas and to admit the deuteron beam to the target chamber.

The SiO windows used in the experiment were 5–10 $\mu\text{g}/\text{cm}^2$ (about 300 atoms thick) and were made by evaporating SiO onto a thin Zapon backing which was later removed by bombarding the film in the ion

beam of the accelerator. The SiO films have been discussed more fully elsewhere.¹¹ The windows were glued to their holders with dextrose. In the early stages of this work much difficulty was experienced with windows rupturing when exposed to the beam under vacuum conditions, for example, during a deceleration. The rupturing was completely overcome by having a supply of electrons ($\sim 1 \mu\text{a}$) available from a small tungsten filament during deceleration operations. With gas in the chamber, no auxiliary electron supply was required.

Electrons were removed from the window both by being pushed out by the beam and by charge exchange. When the window became charged in this way, the beam was decelerated in approaching it. Thus dE/dx was changed, as was the energy loss. By measuring this change in stopping power, and referring to Fig. 4, it was possible to estimate the potential reached by the window with the electron supply cut off. In one such case the potential was calculated to be 2 kv. The rupturing was attributable to electrostatic forces.

The scattering and straggling in these films which depended on the nature of the film had a bearing on the interpretation of the results of this experiment. For if the observed straggling of, say, 300 ev in a film of stopping power 3.5 kev were the result of variations in thickness, it would follow that the least scattered deuterons would have come from the thin parts of the film and on the average would have had more energy than the more widely scattered deuterons. Since the decelerator on which the energy measurements are based accepted only a narrow pencil of deuterons (estimated semiangle 0.8°), a systematic overestimate of the mean deuteron energy could have arisen. There were two independent reasons for believing that such did not occur.

The films were prepared by evaporating SiO from a tungsten coiled filament onto a Zapon film about 15 cm away in vacuum. Knowledge of the actual density of the films, in SiO atoms/cm², was based only on the geometry of the evaporation of a weighed amount of SiO and on weighing extensive films deposited on mica sheets. These methods agreed to 20 percent and gave an estimated surface density of $1.4 \pm 0.2 \times 10^{17}$ SiO molecules/cm².

The following types of film can be identified:

- (1) Pure SiO films, prepared by washing off the Zapon backing. These are tiresome to prepare.
- (2) SiO films in which the Zapon backing had been largely driven off by deuteron bombardment.
- (3) SiO films of either of the above types, in which appreciable (~ 500 ev) growth had occurred presumably because of the deposition of carbon films from the residual gas.

When decelerator current was plotted against energy for films of type (1), a Gaussian distribution was obtained; in fact, the data appeared as straight lines

when plotted on probability paper. These films showed an essentially constant relation between energy loss ΔE and straggling S , where S is defined as the interval which includes half the current on either side of the peak of the Gaussian distribution.

Films of type (1) gave the data shown in Table I (30-keV incident deuterons). If the film were uniform, and if the straggling arose from the fluctuations in the number of interactions N , then

$$S/\Delta E = 0.674N^{1/2}/N,$$

and $N = (0.674\Delta E/S)^2$. This equation gives for the three films above, $N = 181, 158, 153$, and the energy per interaction $\epsilon = 39, 33, 31$ eV, respectively.

Such consistent behavior suggests that the films were uniform. Films of type (2) are believed to retain a skeleton of decomposed Zapon, which contributes one-third of the total stopping power. These films were similar to type (1) films in their relation between stopping power and straggling. Type (3) films showed a larger $S/\Delta E$, suggesting that the matter deposited under bombardment in vacuum took place non-uniformly. Preferential deposition of this kind has been observed on electron microscope preparations.

Nonuniform carbon deposition has, however, negligible effect on the angular distribution since, for Rutherford scattering, the probability of scattering at θ into $d\theta$ is

$$P(\theta)d\theta = \frac{2Ne^4Z^2z^2 d\theta}{E^2 \theta^3},$$

and most of the scattering is due to Si, the highest Z component. Secondly, an energy analysis of the scattered deuterons has been made by Wenzel (private communication) on a type (2) film using a double focusing spectrometer. Most of the intensity in such an analysis can be identified as due to Rutherford scattering from the Si and O components with only a minor contribution from carbon and an extremely faint trace from tungsten.

Scattering in these films was essentially plural for the least scattered one-third and single for the remainder. A calculation of the scattering in one of these films, by use of the theory of Molière, and a Fermi-Thomas screening model for Si gave a calculated scattering of 40 percent of the observed scattering; and this is all that can be expected, considering the modest resolving power of the scattering measurements (1.2°) and the uncertainty in density and composition of the films.

Beam Measurement

In the design of this experiment, all particles incident upon the thin window passed through target gas which was visible from the proportional counters. Thus the whole target chamber could be made a Faraday cup, and the chamber was insulated for this purpose. To

TABLE I. Energy straggling in SiO films.

	Energy at $\frac{1}{2}$ intensity, eV	Energy at $\frac{1}{2}$ intensity, eV	Energy at $\frac{1}{2}$ intensity, eV
Film I	7450	7080	6740
Film II	5420	5140	4870
Film III	5020	4770	4500

translate the current measured to the target chamber into incident particles, the following precautions had to be observed.

A. Stray Currents

Conduction between target chamber and ground was made negligible by good insulation. An appreciable electron current was found from electrons knocked out of the window by the incoming beam and was suppressed by a negatively charged electrode between window and beam defining slit. The potential required to suppress the current was proportional to the energy of the incoming beam; 1 v of suppression per kilovolt of beam energy reduced it to zero. Deuterons scattered from the window or through the window from the interior of the target chamber were not suppressed and, by calculation, should have been quite negligible.

Undesired parts of the incoming beam were removed by the 5-mm defining slit, the edges of which were sharp enough so that there should have been no appreciable scattering at these energies. Another source of spurious charge was the selective collection of ions produced by the beam in the residual gas of the vacuum outside the window. The target chamber was held 10 to 16 v positive with respect to ground by the current integrator and hence could have collected negative ions from this region. However, the electron suppression electrode was 100 to 150 v negative and could have collected positive residual gas ions from the same regions so that the positive current to it gave an indication of the error from this source. The error was quite negligible.

B. Corrections for Neutralized Deuterons in the Beam

A fraction of the beam incident on the target was neutral because of charge exchange with the residual gas between the analyzer magnet and the target chamber and gave reactions although not registering as charge. These reactions were estimated by the following procedure. The incident beam was adjusted until it was as steady as possible, and three runs were made. The first and third were made with both charged and neutral particles entering the target whereas the second was made with the charged particles being deflected by a neutralization magnet placed directly in front of the SiO window so that only neutrals entered the target. From the data for these three runs the percentage of neutrals was calculated. The accuracy of the measurement of the percentage of neutrals was only 10 percent, but, since the neutral beam was, at most, 5 percent of the charged beam, there was an uncertainty

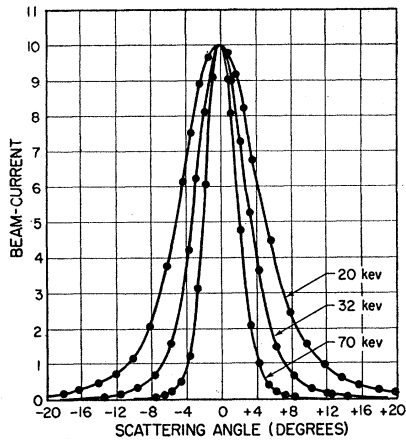


Fig. 6. Scattering in a typical SiO foil.

of less than ± 0.5 percent in the total number of incident particles. At the lower energies, some negatively charged deuterons were produced; and these, if numerous, could have produced an error in the beam current measurement since the method used to detect neutrals did not indicate the presence of negatives. Measurements of the positive-neutral-negative ion proportion as a function of energy, made in another apparatus, show that the energies do not go low enough in these correction measurements for the negative ions to reach significant proportions.

C. Beam Contamination

For most of the data the mass-2 beam spot was used, and contamination of the D^+ ions with H_2^+ had to be considered. However, as discussed previously, the ion source used produced over 10 times as many atomic ions as molecular ions, and, since the deuterium used contained less than 1 percent hydrogen, the H_2^+ should have been less than 0.1 percent of the mass-2 beam. A check was made by the comparison of cross sections obtained with mass-2 and mass-4 beam; these checked within the statistical error of 1.5 percent.

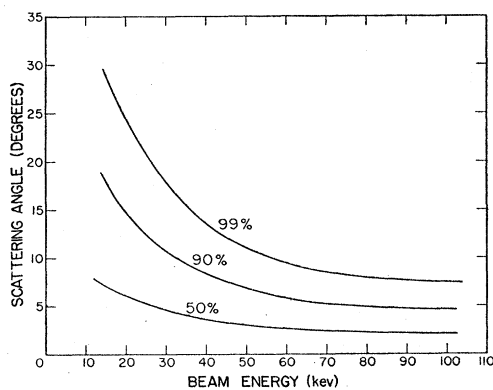


FIG. 7. Semiangle of the cones which include 50, 90, and 99 percent, respectively, of the total beam transmitted by a typical SiO window, as a function of energy.

D. Current Integrator

The current integrator used has been described elsewhere.¹² It was not absolute and so was calibrated with a potentiometer and a standard resistor. Calibrations had an internal consistency of 0.3 percent. The absolute accuracy appears to be 0.5 percent for currents above $0.04 \mu a$.

Counters

The counters were 2 in. in diameter and 6 in. long, with a 2-mil central wire, and were operated in the proportional region. Two counters were used simultaneously (with separate amplifiers and scalers) for the purpose of detecting and correcting for possible asymmetry in the primary beam. For one counter, the geometry was sensitive to such displacements. Both counters were used throughout the experiments, although the counts observed in the two channels turned out to be the same, within statistics, so that the double counter precautions were not needed.

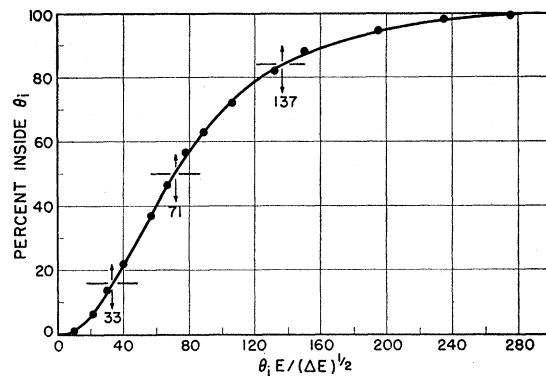


FIG. 8. Percent of beam included inside angle θ_1 .

The counter window thicknesses and gas pressures were adjusted to give optimum discrimination for the wanted particles in each case and are given under the separate headings.

Counter pulses from each counter were recorded separately with a Los Alamos Model 101 amplifier and a Model 750 scaler. At a counting rate of 1000/sec, counting losses caused by the insensitive time of the amplifier after a pulse amounted to 0.2 percent. Accordingly, counting rates were always kept below 1000/sec.

Solid Angle and Path Length

The length of the paths of the deuterons in the target volume and the solid angle of acceptance of the counters at different points along the path varied with the inclination and orientation of the beam path. It was first necessary to know the angular distribution of the beam as scattered by the window. This was measured by building an apparatus in which an arm with a small

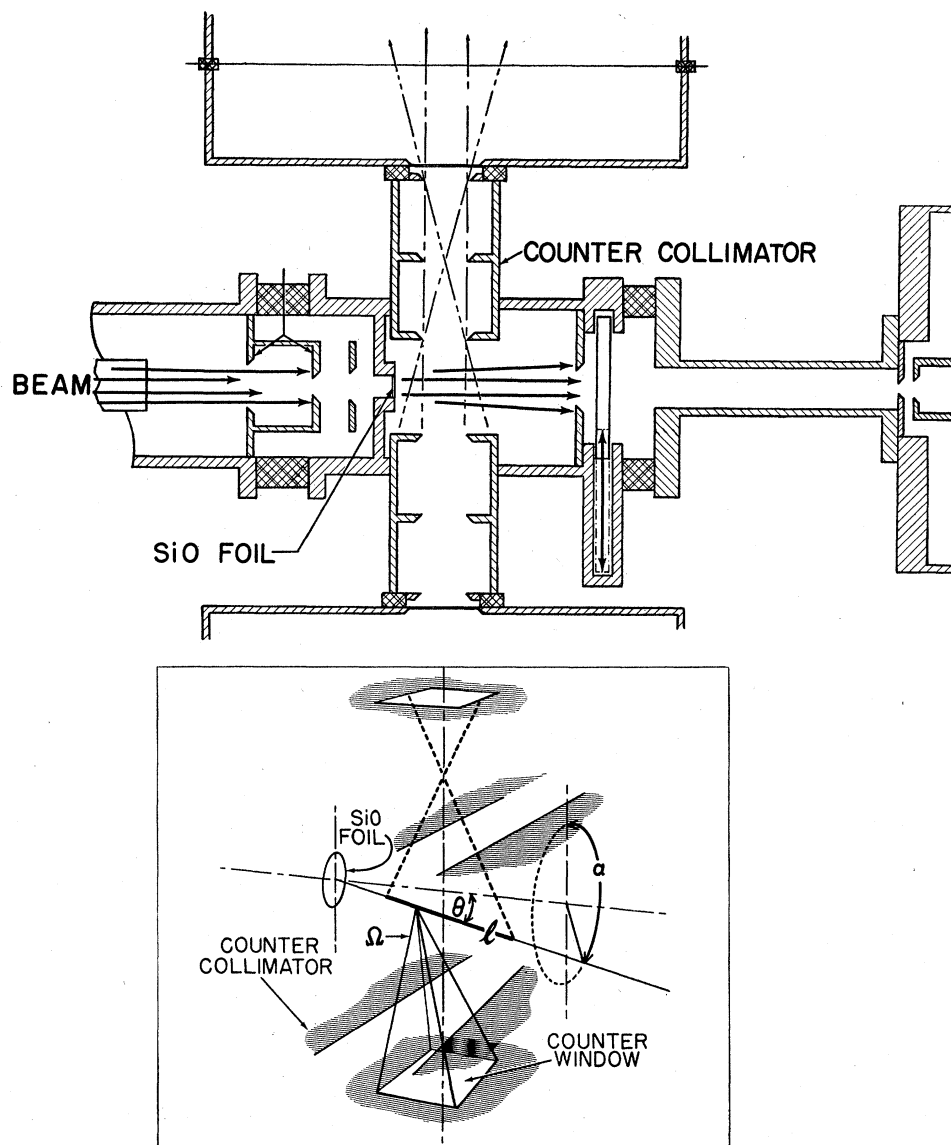


FIG. 9. Schematic diagram of target chamber showing geometry.

shielded Faraday cup rotated about the center of the window as an axis. The current collected by this cup as a function of scattering angle θ gave data of the type shown in Fig. 6. A series of such curves taken at various energies was translated into curves showing how the percentage of beam current included inside a given angle varies with energy (Fig. 7).

In these measurements, the angular resolving power was of the order of 1.2° , and an unscattered beam would have had an angular half-width of 1.1° at half-maximum.

For application of these scattering measurements to the solid-angle correction, it was necessary to construct a universal curve from which the divergence produced

by windows of differing thicknesses could be read off at various energies.

It was found experimentally that the data could be well represented by a universal curve (Fig. 8) in which intensity was plotted against $(E/\Delta E^3)\theta$, where ΔE is the energy loss in the film measured at a standard 30-kev energy, and, therefore, a measure of the film's thickness and E was the average deuteron energy in the window.

In application of the universal scattering curve to the correction, for counter solid angle, the approximation was made that the distribution could be represented by scattering at three angles, θ_1 , θ_2 , and θ_3 , each containing one-third of the total beam (this approximation was considerably better than needed to keep within the desired accuracy). From the curve in Fig. 8, one

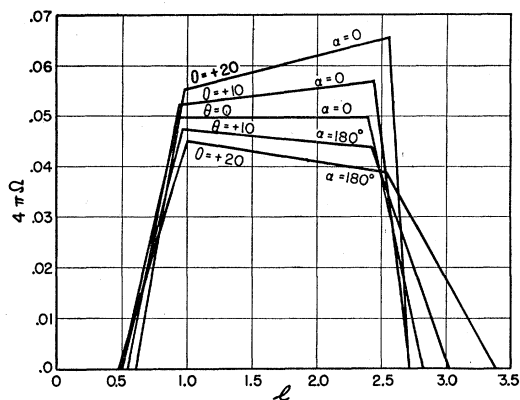


FIG. 10. Solid angle subtended by the counters as a function of distance from the SiO window along the beam for several angles of inclination of beam to axis.

finds that

$$\begin{aligned}\theta_1 &= 33(\Delta E)^{1/2}/E, \\ \theta_2 &= 71(\Delta E)^{1/2}/E, \\ \theta_3 &= 137(\Delta E)^{1/2}/E.\end{aligned}$$

Thus for any given run, knowing ΔE and E , three average angles representing the scattering could be calculated.

The next step was to calculate the average solid angle and target path length as a function of θ , the divergence.

Using the geometry of Fig. 9, the value of Ω was calculated algebraically for points on any particular ray of inclination to the axis θ and azimuthal angle α as a function of distance along the ray l . Figure 10 shows such Ω plotted against l for three inclinations: $\theta = 0^\circ, 10^\circ, 20^\circ$; $\alpha = 0^\circ$ and 180° (corresponding to going toward one counter and away from it). Similar curves were prepared for oblique pencils, $\alpha = 45^\circ$ and 135° and $\alpha = 90^\circ$. By summing the areas over $\alpha = 0^\circ, 45^\circ, 90^\circ, 135^\circ,$ and 180° and averaging for the two counter-slit systems (which differed by mechanical tolerances), an average value of Ωl was obtained for a given value of θ . Figure 11 shows the resulting Ωl averages as a function of θ .

It turned out that this geometrical factor Ωl is insensitive to θ over the range zero to 30° , varying only 2 percent. At $\theta = 32^\circ$, Ωl jumped by nearly 10 percent, and this occurred when particles passed inside the counter-slit system. In these experiments few particles were scattered out to $\theta = 32^\circ$. From Fig. 7, at 20 kev we see that in one particular case 99 percent of the beam lay within $\theta = 25^\circ$ for beam energy 20 kev.

These linear approximations to nonlinear functions used in calculating the effect of scattering were more than sufficiently accurate since the whole correction to Ωl because of the scattering was only 1 percent, and the uncertainty in Ωl because of other factors was larger. The corrections are included in this report mainly

because it was not immediately obvious that the correction for divergence would be so small.

Errors

An effort was made to keep the errors in the experiment as small as possible. In Table II the errors are listed under five headings: number of incident particles, number of target atoms, number counted, solid angle, and energy. Values listed under energy are the errors in voltage translated into errors in cross section by use of an empirical formula for the cross-section curve. The experiment was designed to go down to 20-kev deuteron energy, and, as may be seen from the table, the accuracy falls off rapidly below 20 kev.

The standard error (the root of the sum of the squares) which appears at the bottom of each column was based on the assumption that each of the individual errors is Gaussian in character. Such was most probably not the case; therefore, the error assigned was arbitrarily twice this.

ABSOLUTE DETERMINATION OF THE $D(d,p)T$ REACTION CROSS SECTION

In the deuteron-deuteron reactions, there are three resultant charged particles, H, T, and He^3 , which can be detected by a proportional counter. It was necessary then to identify positively each of the counter pulse groups with the corresponding reaction particle and to count only the desired group. For the $D(d,p)T$ branch, it was determined that the tritons could conveniently be detected with the counters filled with argon to a pressure of 10 cm of mercury, with mica windows 1.5 mg/cm² thick, and operated with 550 v on the center wire. Under these conditions, He^3 particles from $D(d,n)\text{He}^3$ did not get through the window, protons from $D(d,p)T$ lost 120 kev energy in the counter gas, and tritons lost 270 kev. Tritium contamination in the target would have produced α 's which would have lost 1.9 Mev in the counter gas. A pulse-height analyzer was used to examine the pulse-height distribution of the counters. The tritons were well resolved from the protons. The protons were poorly resolved from the

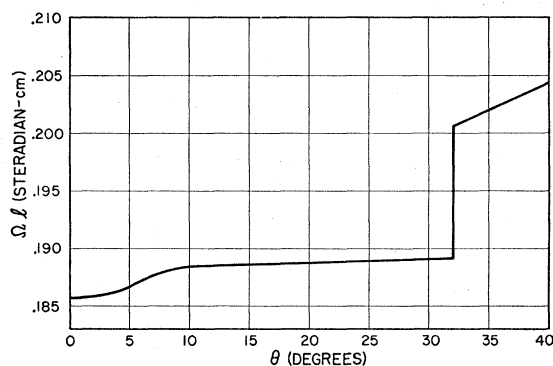


FIG. 11. Product of solid angle subtended by the counters and beam path length as a function of scattering angle.

TABLE II. Errors.

	D(<i>d,p</i>)T and D(<i>d,n</i>)He ³			T(<i>d,n</i>)He ⁴			He ³ (<i>d,p</i>)He ⁴		
	25 kev (%)	50 kev (%)	100 kev (%)	10 kev (%)	25 kev (%)	50 kev (%)	100 kev (%)	40 kev (%)	80 kev (%)
1. Number of incident particles									
<i>a.</i> Current integrator	0.5	0.5	0.5	0.5	0.5	0.5	0.5	0.5	0.5
<i>b.</i> Neutralized beam	0.3	0.1	0.1	0.5	0.3	0.1	0.1	0.2	0.1
<i>c.</i> Secondary particles	0.3	0.3	0.3	0.3	0.3	0.3	0.3	0.3	0.3
<i>d.</i> Beam contamination	0.1	0.1	0.1	0.1	0.1	0.1	0.1	0.1	0.1
2. Number of target atoms									
<i>a.</i> Pressure	0.5	0.5	0.5	0.5	0.5	0.5	0.5	0.5	0.5
<i>b.</i> Gas purity	1.0	1.0	1.0	2.0	1.0	1.0	1.0	1.0	1.0
<i>c.</i> Temperature	0.1	0.1	0.1	0.1	0.1	0.1	0.1	0.1	0.1
3. Number counted									
<i>a.</i> Efficiency of counters	0.2	0.2	0.2	0.2	0.2	0.2	0.2	0.2	0.2
<i>b.</i> Statistics	1.7	0.7	0.8	0.5	0.2	0.1	0.1	1.7	0.4
4. Solid angle									
<i>a.</i> Beam not central	0.3	0.3	0.3	0.3	0.3	0.3	0.3	0.3	0.3
<i>b.</i> Measurement of slit system	0.3	0.3	0.3	0.3	0.3	0.3	0.3	0.3	0.3
<i>c.</i> Error in calculation approximations	0.2	0.2	0.2	0.5	0.2	0.2	0.2	0.2	0.2
5. Energy									
<i>a.</i> High-voltage measurement	0.4	0.2	0.1	0.6	0.4	0.3	0.1	0.6	0.4
<i>b.</i> Variation in high voltage	0.4	0.2	0.04	1.6	0.4	0.2	0.03	0.2	0.1
<i>c.</i> Spread in particle energy	0.3	0.1	0.03	0.4	0.3	0.1	0.02	0.1	0.1
<i>d.</i> Film thickness	0.6	0.3	0.07	3.0	0.7	0.3	0.05	0.3	0.2
<i>e.</i> Energy loss in gas	0.7	0.3	0.05	3.0	0.7	0.3	0.05	0.4	0.2
Standard error	2.5	1.6	1.6	5.3	1.8	1.5	1.4	2.4	1.5
Assigned error	5.0	3.2	3.2	10.6	3.6	3.0	2.8	4.8	3.0

noise. A very small counting rate of α particles from T(*d,n*)He⁴ showed that there was a slight tritium contamination. At these bombarding energies the protons and tritons came off in almost opposite directions. Since the top and bottom counters were located opposite each other, it was possible to count these pairs of reaction particles in coincidence when both particles entered the counters. Coincidences did occur and gave a check on the identification of the particles.

The one other reaction particle which could be detected in the counters was the neutron from the D(*d,n*)He³ branch. This neutron had an energy of 2.47 Mev and could cause recoils in the gas of the counters. To measure the number of these recoils, the counters were provided with brass shutters which could be drawn across the counter windows to prevent any charged particles from entering the counter. It was found that 0.3 percent of the pulses assigned to the tritons were from neutron recoils, and the number of tritons detected was so corrected.

The target gas, deuterium, was supplied from a small uranium reservoir, from which it was admitted to the target by careful heating. The pressure in the target was controlled by means of needle valves. A sample of gas was taken from the target before running for analysis on a mass spectrometer to obtain the initial purity. Another sample was taken and analyzed at the completion of a half-day of running to obtain the final purity. The variation in purity was then interpolated linearly with bombardment time.

Before and after each series of runs, the thickness of the window was measured with the decelerator at a high voltage of E_0 . Then, with deuterium gas in the

target, runs were made at a series of different high voltages, but always beginning and finishing with runs at E_0 . At each high voltage three runs were made, first with the total analyzed beam entering the target, second with the charged part of the beam deflected so as to determine the neutral component, and third with the total beam again. For each run, the time, target pressure, and temperature at the beginning and end of the run, the high voltage, the integrated beam current, and the number of triton counts from each counter were recorded.

The mean energy in the target was calculated for any particular run by subtracting from the high voltage one-half the gas thickness and the window thickness at the energy of the run. The window thickness was computed from the thickness at E_0 , interpolated for the midtime of the run, by means of the thickness *vs* energy curve of Fig. 4.

The density of the target nuclei, in number per cubic centimeter, was calculated by the equation

$$N_t = CmN_0PT_0/V_0P_0T,$$

where C = the purity of the deuterium gas, m is the number of atoms per molecule (2 for deuterium), N_0 = Avogadro's number, P and T are the pressure and absolute temperature of the gas, and V_0 is the molar volume at pressure P_0 and temperature T_0 . The number of incident deuterons was calculated by the relation:

$$n_i = q/[e(1-\nu)],$$

where q is the integrated beam current in coulombs, e is the electronic charge in coulombs, and ν is the fraction of the total beam that is neutral. The differential

TABLE III. Cross sections derived from smoothed curves.

Deuteron energy (keV)	D(<i>d,p</i>)T (millibarns)	D(<i>d,n</i>)He ³ (millibarns)	T(<i>d,n</i>)He ⁴ (barns)	He ³ (<i>d,p</i>)He ⁴ (millibarns)
7.5			0.000275 ^a	
9.0			0.000939 ^a	
13.0	0.0352	0.0329	0.00780 ^a	
19.0	0.213	0.200	0.0448 ^a	
22.0	0.391	0.367	0.0859	
25.0	0.629	0.592	0.144	
30.0	1.14	1.08	0.278	
33.0	1.54	1.46	0.394	
36.0	1.98	1.88	0.519	0.124
40.0	2.56	2.43	0.723	0.258
46.0	3.58	3.42	1.11	0.605
53.0	4.98	4.78	1.62	1.28
60.0	6.50	6.25	2.18	2.32
67.0	8.14	7.86	2.82	3.84
73.0	9.59	9.30	3.36	5.65
80.0	11.2	10.9	3.93	8.45
93.0	13.9	13.6	4.74	16.2
100.0	15.4	15.2	4.90	
107.0	16.5	16.6	4.95	
110.0	17.1	17.0	4.95	
113.0	17.5	17.4	4.94	
120.0			4.70	

^a Derived from extrapolated Gamow curve.

reaction cross section at 90° was then calculated by the equation

$$(d\sigma/d\omega)_{90^\circ} = Y/(Nn\epsilon w),$$

where Y is the total number of triton counts in both counters and w is the average geometry of counting for the two counters in steradian-cm. Finally the total cross section was computed by the formula

$$\sigma_{\text{total}} = 4\pi gh(E)(d\sigma/d\omega)_{90^\circ},$$

where g is the correction factor to the counter solid angle for motion of the center of mass, and $h(E)$ is the correction factor for the angular anisotropy of the reaction products in the laboratory system. The correction g was applied although its maximum value was only 1.02. The factor $h(E)$ has the form

$$h(E) = \frac{1}{1 + \frac{1}{2}C_2 + \frac{3}{8}C_4 + [(3/2)C_2 + (30/8)C_4]p^2},$$

where C_2 and C_4 are experimentally determined coefficients in the Legendre polynomial expansion of the anisotropy, taken from Wenzel and Whaling,⁷ and

$$p^2 = \cos^2\theta = 3E/(8000 + E),$$

where θ is the center-of-mass angle that corresponds to 90° in the laboratory system and E is the energy in kev.

Values of the total cross section as a function of energy for the reaction D(*d,p*)T are given in Table III. A plot of the total cross section as a function of energy for the reaction D(*d,p*)T is shown in Fig. 12. The lowest energy at which the cross section was measured was determined by a balance between the low yield and the growth of the SiO windows, i.e., the longer running time

required to obtain a sufficient number of counts caused greater uncertainty in the determination of the energy loss in the SiO window.

THE D(*d,n*)He³ CROSS SECTION

Although the D(*d,n*)He³ reaction can be detected by counting either neutrons or He³ particles, the latter can be counted with higher precision because of their charge. The He³ particles have a range in air of only 0.4 cm; therefore, thin counter windows made of Zapon, of 0.1-cm air equivalent, were used. The counters were filled with an argon-CO₂ mixture to a pressure of 3 cm of mercury. The He³ particles and the tritons from the D(*d,p*)T reaction were well separated from each other in pulse height and from noise. The He³ particles were stopped in the counter gas whereas the tritons passed through the counter volume. This provided a test of the identification of the pulses, for the He³ particles gave not only the larger pulses but their pulse heights were not appreciably changed by small changes in counter gas pressure whereas the triton pulses were almost proportional to the pressure. No coincidences should occur between the tritons in one counter and He³ particles in the other, and none was observed.

The thin Zapon windows had a serious disadvantage in that it was impossible to make them gas-tight, and the deuterium gas in the target chamber quickly became contaminated with argon. At the higher bombarding energies the deuterons in the beam were scattered by the argon with enough energy to penetrate the counter windows. These deuterons gave a large number of small pulses, and pile-up of these pulses occurred which rendered the counters inoperable when the argon contamination became high. An absolute determination of the cross section was attempted at a few energies, but, because of the uncertainty in the knowledge of the target gas composition and difficulties in counting, the accuracy was poor.

A better procedure was found to be to measure the 90°

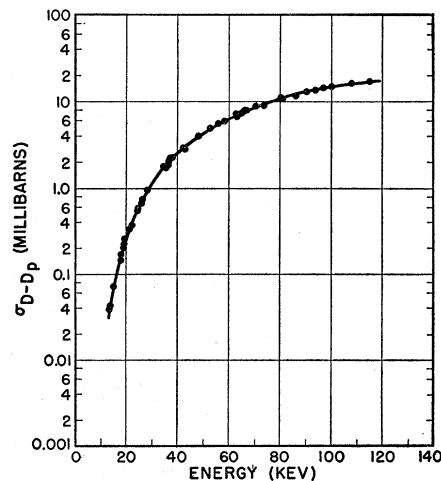


FIG. 12. D(*d,p*)T cross section.

yields for the two reactions $D(d,p)T$ and $D(d,n)He^3$ by counting tritons and He^3 particles simultaneously and combining this ratio with the previously determined $D(d,p)T$ cross section to give that for $D(d,n)He^3$ branch.

Such a procedure had the advantage that since the ratio is essentially independent of target gas parity and density, a constant stream of target gas could be used, which swept out argon contamination and reduced scattering to acceptable limits. The $D(d,n)He^3$ cross section derived from this ratio, assuming similar angular distributions for the two branches, is given in Table III.†

The results are shown in Fig. 13. Each point plotted represents the average of about five experimental determinations. The ratio at 20 kev is 0.94 and it increases with increasing energy to a value of 0.99 at 100 kev. The $D(d,n)He^3$ cross section, derived from this ratio and the measured $D(d,p)T$ cross section, is presented in Table III, as is the total cross section.

The resulting total cross section is shown on a Gamow plot in Fig. 14. If the finite height of the Coulomb

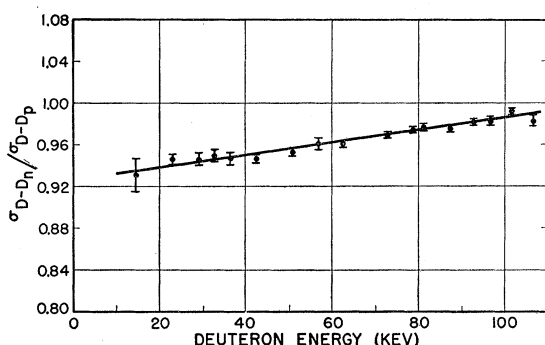


FIG. 13. Ratio 90° yield $D(d,n)He^3/D(d,p)T$ vs energy.

barrier is allowed for,¹⁴ this introduces a departure from the zero energy slope ($44.4 \text{ kev}^{\frac{1}{2}}$) amounting to 0.2 percent at 10 kev and 7.2 percent at 100 kev. The best straight line was drawn through the experimental points, with a slope of 45.8, i.e.,

$$\sigma = \frac{2.88 \times 10^2}{E} \exp(45.8E^{-\frac{1}{2}}) \text{ barns,}$$

with E in kev.

THE ABSOLUTE DETERMINATION OF THE $T(d,n)He^4$ CROSS SECTION

Tritium gas was used as the target. It was supplied from a small uranium reservoir and after use was collected into another uranium trap. About one-third of the gas for each filling was taken as a sample for analysis. Analyses were made on a mass spectrometer before and after use.

† Note Added in Proof.—Eliot, Roaf, and Shaw, [Proc. Roy. Soc. (London) A216, 57 (1953)], report markedly differing angular distributions for the two branches, based on observations at two angles, $90^\circ \pm 15^\circ$, and $125^\circ \pm 15^\circ$.

¹⁴H. Bethe, Revs. Modern Phys. 9, 163 (1937).

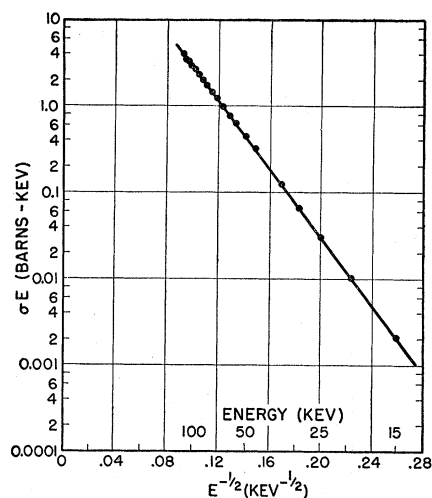


FIG. 14. Gamow plot of total $d-D$ cross section.

The number of reactions taking place was determined by counting the α particles resulting from the reaction. The counters were filled with argon gas to a pressure of 10 cm of mercury and were operated with 550 v on the center wire. The counter windows were of mica 1.5 mg/cm² thick. The α -particle pulses were so much larger than pulses from anything else that the background was negligible.

The experimental procedure was the same as in the case of the $D(d,p)T$ reaction. The calculation of the total cross section differed only in that it was assumed that the α particles were given off isotropically in the center-of-mass system, as based on the results of Bretscher and French,⁸ so that

$$\sigma = 4\pi (d\sigma/d\omega)_{90^\circ}.$$

The experimental results for this cross section are listed in Table III and are shown in Fig. 15 with a smooth curve drawn through most of the points. The peak of the cross-section curve, around 107 kev,

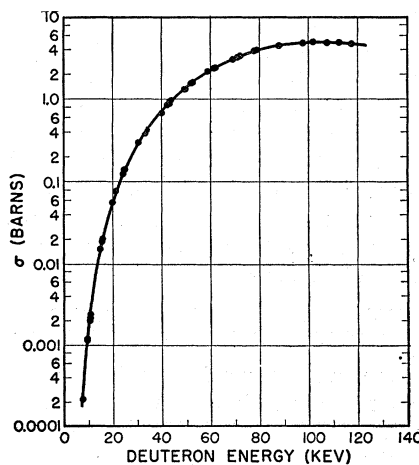


FIG. 15. $T(d,n)He^4$ cross section.

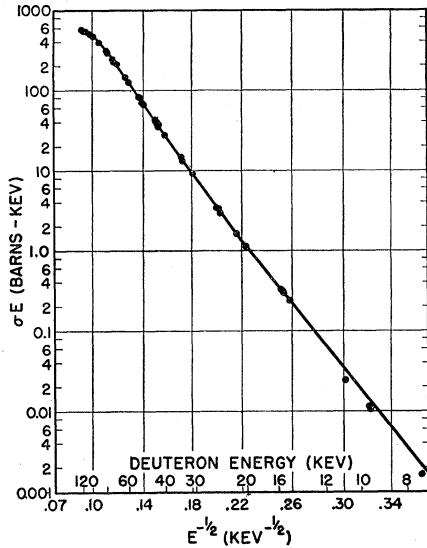


FIG. 16. Gamow plot of cross section $T(d,n)He^4$.

is quite broad. The accuracy in selecting the peak energy is somewhat limited because of the high-voltage limitations of the equipment. The smooth curve lies above the experimental points at the energies 7, 9, and 11 keV because failure of the counter collimating system and excess production of condensable vapor gave good reason to expect that the experimental value of the cross sections at these energies might be low.

A Gamow plot of the results is given in Fig. 16. Since angular anisotropy has not been detected, it is reasonable to assume an S -wave interaction which leads to a cross section with a dependence on energy, at energies remote from the resonance, of the form

$$\sigma = (A/E) \exp(-2\pi e^2/\hbar v) = (A/E) \exp(-44.40E^{-1/2}),$$

where e is the electronic charge and v is the relative velocity of the nuclei and the deuteron energy E is expressed in keV. When $\log E\sigma$ is plotted against $E^{-1/2}$ (Fig. 16), the points lie on a smooth curve which merges asymptotically into a straight line. The points below 16 keV were neglected, and the asymptote through the remaining lowest points, 20 and 16 keV, was drawn with the theoretical slope of 44.40 keV^{1/2}. Since, as the energy is reduced, the validity of the theory should improve and at the same time the experimental errors increase, especially the liability to systematic error, it is felt that there is some justification for neglecting the values below 16 keV which fall appreciably below the Gamow theoretical curve.

THE RATIO OF THE CROSS SECTIONS FOR THE REACTIONS $T(d,n)He^4$ AND $D(d,p)T$

There were two reasons for making an independent measurement of the ratio of the cross sections for the reactions $T(d,n)He^4$ and $D(d,p)T$: (1) the ratio obtained from the absolute measurements reported here is in rather serious disagreement with previous measure-

ments;¹ (2) the ratio measurement provided a test of the internal consistency of the separate cross-section measurements.

In this experiment the α particles from the $T(d,n)He^4$ reaction and the tritons from the $D(d,p)T$ reaction were counted simultaneously, by use of a known mixture of tritium and deuterium gas as a target. The ratio of the counting rates for these two particles, when corrected for the concentrations of the gases in the mixture, gave the ratio of the cross sections directly. This measurement, as in the previous ratio experiment, was independent of the beam current and pressure and temperature of the target gas.

For obtaining the comparable counting rate required for minimum error from the two reactions, it was necessary to have a gas mixture containing a relatively small proportion of tritium since the cross section of tritium is about 350 times larger than the deuterium cross section. A gas mixture was prepared by mixing accurately known volumes of the two gases in the ratio of 400 volumes of deuterium to 1 of tritium. The ratio of gas concentrations was known to within about 0.5 percent. However, at least two factors changed the ratio of the gases in the target chamber. To avoid breaking the fragile SiO window, it was necessary to admit the gas to the target chamber slowly through a needle valve. Fractionation occurred in the needle valve by selective diffusion so that early samples from the gas reservoir were enriched in deuterium, whereas later samples were enriched in tritium. This fractionation was greatly reduced by inserting a small reservoir between the main reservoir and target chamber which could be filled to the full pressure of the reservoir and then emptied completely through the needle valve into the target chamber. Also, the SiO windows in the target chamber had small leaks into the high vacuum, and fractionation occurred at these leaks because deuterium leaked through more readily than tritium. Because of this, the gas in the target chamber was progressively enriched in tritium. These fractionation effects reduced the accuracy of the ratio measurement.

Both the α particles from the $T(d,n)He^4$ reaction and

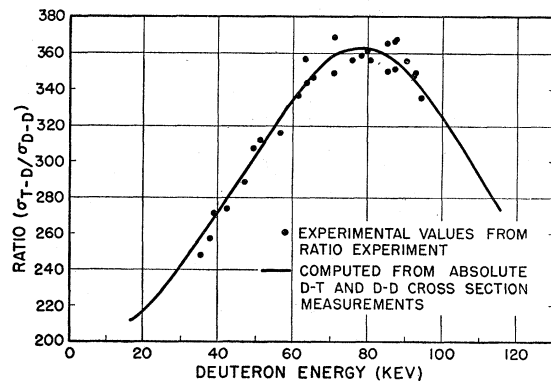


FIG. 17. Ratio 90° yield $[D(d,n)He^4]/90^\circ$ yield $[D(d,p)T]$ vs energy.

the tritons from the $D(d,p)T$ reaction were counted simultaneously. The counters had mica windows, 1.5 mg/cm^2 thick, and were filled with argon to a pressure of 10 cm of mercury. There was good separation in pulse height between the α pulses and triton pulses and from background.

The experimental values for the ratios are shown by circles in Fig. 17. The smooth curve is the result of dividing the experimental values of the cross section of the $T(d,n)He^4$ reaction by those of the $D(d,p)T$ reaction reported here. The agreement between the measured ratio and the ratio of the absolute measurements is within 1.5 percent.

THE CROSS SECTION FOR THE REACTION $He^3(d,p)He^4$

For this experiment, pure He^3 gas was used in the target chamber at a pressure of 1 mm of mercury, supplied from a glass flask through a needle valve. Samples of the gas were analyzed with the mass spectrometer, as in the case of deuterium and tritium above. The number of reactions was determined by counting the 14-Mev protons resulting from the reaction because if α particles had been counted, they would have been indistinguishable from the α particles resulting from possible tritium contamination. The counter windows used were 0.035-in. thick Al. The windows were so thick that there was no possibility of confusion in the identification of the particles since only penetrating particles such as 14-Mev protons could get through the windows. The protons lost 90 percent of their energy in the windows and were then stopped in the counters, which were filled to 1 atm with argon. The experimental procedure and the treatment of data are similar to that reported above. In calculating

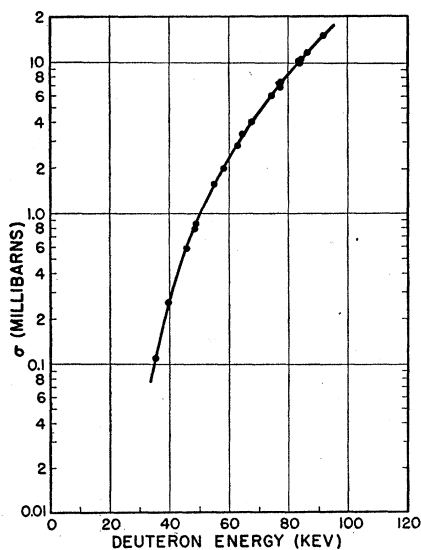


Fig. 18. $He^3(d,p)He^4$ cross section.

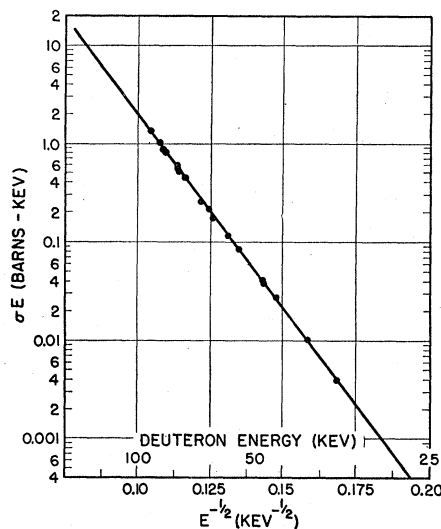


Fig. 19. Gamow plot of $D(He^3,p)He^4$ cross section.

the total cross sections from the measured differential cross sections at 90° the angular distribution was assumed to be isotropic in this energy region.¹⁰

A plot of the cross section as a function of the energy of the incident deuteron is shown in Fig. 18 and the results tabulated in Table III. The lowest energy at which the cross section was measured was fixed by the background, which became objectionable at low counting rates, whereas the highest energy was the maximum available energy of the accelerator used.

A Gamow plot of the data (Fig. 19) is linear with a slope of $91.0 \text{ keV}^{\frac{1}{2}}$. The simple penetrability gives a slope of 88.80, within 2.5 percent of the experimental value.

Although nuclear cross sections conventionally refer to interactions between bare nuclei, laboratory measurements such as these refer to interactions in which at least one of the partners is a neutral atom (or part of a molecule). This verges on significance at these energies, for an energy E in the lab system is equivalent to $E + Ze^2/\bar{r}$ (\bar{r} is the effective radius of the electron cloud) in the conventional system. Ze^2/\bar{r} amounts to 26 eV for H or 87 eV for He. Expressed as a correction to the cross section, this amounts to -2.6 percent for $\sigma_T(d,n)He^4$ at 10 keV and -2.7 percent for $\sigma_D(He^3,p)He^4$ at 35 keV.

The data presented in this paper do not include this correction.

The authors acknowledge with pleasure the assistance of E. Fermi and R. L. Garwin, who called the problems to our attention and had an important share in formulating the experiment; H. Agnew, who contributed to the design of the apparatus; W. Ogle, who suggested the deceleration technique; J. H. Coon, who designed the gas handling apparatus and advised in that field; B. B. McInteer, who provided the mass spectrographic analyses; and W. Jones, who prepared the tritium-deuterium gas mixture.